HHS Public Access

Author manuscript

Anal Chem. Author manuscript; available in PMC 2023 August 02.

Published in final edited form as:

Anal Chem. 2022 August 02; 94(30): 10824–10831. doi:10.1021/acs.analchem.2c01814.

Surface Activity of Amines Provides Evidence for Combined ESI Mechanism of Charge Reduction for Protein Complexes

Thomas E. Walker,

Arthur Laganowsky,

David H. Russell*

Department of Chemistry, Texas A&M University, College Station, TX 77843

Abstract

Charge reduction reactions are important for native mass spectrometry (nMS) because lower charge states help retain native-like conformations and preserve non-covalent interactions of protein complexes. While mechanisms of charge reduction reactions are not well understood, they are generally achieved through addition of small molecules, such as polyamines, to traditional nMS buffers. Here, we present new evidence that surface active, charge reducing reagents carry away excess charge from the droplet after being emitted due to coulombic repulsion, thereby reducing the overall charge of the droplet. Furthermore, these processes are directly linked to two mechanisms for electrospray ionization, specifically the charge residue and ion evaporation models (CRM and IEM). Selected protein complexes were analyzed in solutions containing ammonium acetate and selected trialkylamines or diaminoalkanes of increasing alkyl chain lengths. Results show that amines with higher surface activity have increased propensities for promoting charge reduction of the protein ions. The electrospray ionization (ESI) emitter potential was also found to be a major contributing parameter for the prevalence of charge reduction; higher emitter potentials consistently coincided with lower average charge states among all protein complexes analyzed. These results offer experimental evidence for the mechanism of charge reduction in ESI, and also provide insight into the final stages of the ESI and their impact on biological ions.

Graphical Abstract

*Corresponding author: russell@chem.tamu.edu.

Supporting Information

More detailed description of the CC-FEM formation of charge reduced ions. Detailed data for CCS experiments. Mass spectral data for protein complexes in various emitter potential and buffer concentrations conditions. This material is available free of charge at http://pubs.acs.org.

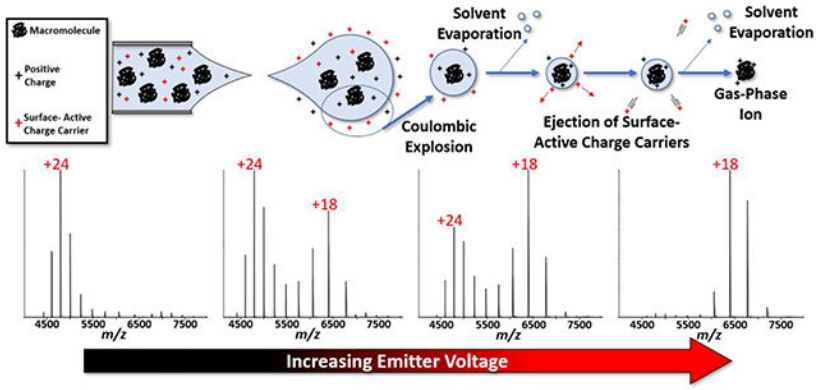

Introduction

Electrospray ionization of biomolecules has gone through many stages of development since it was first described by Fenn and coworkers some 35 years ago.[1–3] But Fenn's vision of the long term impact, expressed in the 1990 review of electrospray ionization "…*that other "cooks"(practitioners) will have even more success than we have had with the recipes to be presented*…" (Fenn et al., page 38)[4] rings true even today! Researchers continue to develop new approaches that improve the informational content of the ESI mass spectral data. Notable examples include super-charging reagents that have played key roles in the development of top-down protein sequencing[5–7] and more recently, the introduction of native mass spectrometry (nMS) buffers that are volatile and reduce salt adduction[8–10] and the use of sub-micron emitters that provide cleaner, more defined mass spectral peaks and better signal-to-noise ratios (S/N).[11–16] While ammonium acetate is an excellent buffer for native MS, other buffer systems are often used to either increase or reduce the charge state distribution of proteins.

Charge reducing reagents are MS-friendly buffers that lower the average charge state (Z_{avg}) of protein ions.[17, 18] Lower charge states appear at higher *m/z* therefore increasing the charge state spacing (resolving power) for ions of proteins and protein complexes. The increased *m/z* separation has proved particularly advantageous for studies of lipid binding to membrane protein complexes[19] and more generally for preserving intact protein complex structures.[20, 21] Lower Z_{avg} is also correlated with more native-like protein states due to less coulombic repulsion throughout the protein structure.[22–24] The most commonly used nMS buffers are ammonium acetate (AmAc), triethylammonium acetate (TEAA), and ethylenediamine diacetate (EDDA) with the latter two being most frequently used as charge reducing buffers.[18, 25] The mechanism of charge reduction and the physicochemical properties that are responsible for observed charge reduction are not well understood. We recently reported results for charge reduction for a series of amino-containing compounds that showed similar charge reduction as TEAA and EDDA, but trimethylamine *N*-oxide (TMAO), showed very different behavior.[19]

The formation of gaseous ions of large molecules from nanodroplets formed by ESI is generally described using the charge residue model (CRM) and ion evaporation model

(IEM).[26–31] The CRM purports that macromolecules acquire excess charges from the evaporating nanodroplet during the late stages of desolvation in the transition from solution to gas-phase ions, whereas IEM is often used to explain ionization of small molecules where the ions are ejected from the droplet due to coulombic repulsion near the surface of the droplet;[27, 30, 32–35] however, neither model accounts for the mechanism of charge reduction in its entirety.

Hybrid models that incorporate both the CRM and IEM processes have been used to explain charge reduction effects observed in ESI formation of ions, most notably, the charge carrier field emission model (CC-FEM).[36–41] Briefly, evaporation of the solvent from the initially formed nanodroplets is adequately described by CRM, but as the solvent evaporates the ion density increases and exceeds the Rayleigh limit resulting in droplet fission and ejection of even smaller nanodroplets. As the solvent loss from the nanodroplet leads to increased coulombic repulsion, an IEM step occurs and surface-active ions are preferentially ejected, thus lowering the total charge of the nanodroplet. These processes proceed stepwise until the transition of solvated ions to solvent-free gas phase ions. Thus, the CC-FEM invokes CRM formation of macromolecular ions to be preceded by an IEM step where surface-active ions (less preferentially solvated) are ejected from the droplet. This model provides increased explanatory power for the formation of charge-reduced macromolecular ions. Clearer understanding of electrospray processes allows for tuning of solution conditions to provide for optimal experimental conditions. Many of the factors outlined above for charge reduction are important for elucidating details concerning structure, stability, and dynamics of protein complexes.

Here, we present recent experimental results for large protein complexes that are consistent with the CC-FEM. Monomeric proteins have been extensively studied via ESI-MS, therefore we have chosen to conduct these experiments on protein complexes which offer to provide a more complex and less well-studied response to charge reduction conditions. A recent example reported by Walker *et al.* revealed remarkable effects of native MS buffers, AmAc and EDDA, on the conformation and stabilities of the GroEL tetradecamer.[42] The protein complexes of C-reactive protein (CRP ~115 kDa), pyruvate kinase (PK ~237 kDa) and glutamate dehydrogenase (GDH ~334 kDa (experimental)) were studied using mixed buffers containing various concentrations of AmAc and TEAA, and the effects of nESI (nano-ESI) emitter potentials were also examined. Higher concentrations of TEAA and higher emitter potentials at each TEAA concentration decreased the Z_{avg} for all proteins. We also examined a series of amino-containing compounds (trimethylamine (TMA), triethylamine, tripropylamine (TPA), 1,5-diaminopentane (1,5-DAP), 1,6-diaminohexane (1,6-DAH), 1,7-diaminoheptane (1,7-DAH)). These reagents were used to examine the effects of surface activity of charge carriers on charge reduction. Increasing the hydrophobicity of the amine compound in the mixed buffer solution corresponded to a decrease in the observed Z_{avg} of all the protein complexes.

Methods

Protein samples of GDH and PK were prepared from lyophilized powders obtained from Sigma. CRP samples were prepared from a 1 mg/mL stock solution obtained from Sigma.

All protein solutions were buffer exchanged using BioRad P-6 size exclusion columns with a mass cutoff of 6000 Da to remove unwanted contaminants from the solution. Protein concentrations varied from 750 nM to 2 μM, depending on the protein used. All amine solutions were used in the presence of 160 mM ammonium acetate (AmAc). All amines were obtained from Sigma. The pH of the AmAc, TMA, TEAA, TPA solutions were pH 6.5 to pH 7. TMA and TPA solutions were acidified slightly using acetic acid to reach pH 6.5. Solutions of the diaminoalkanes 1,5-DAP, 1,6-DAH, and 1,7-DAH were acidified to pH 8 (from pH 9.5 initially) using acetic acid. All pH measurements used 3-color litmus paper purchased from J.T. Baker.

All solutions were sprayed using pulled borosilicate capillaries with an emitter diameter of 1–2 μm. The same tip-pulling program was used across all experiments to mitigate tip diameter effects as much as reasonably possible. Mass spectra were deconvoluted using UniDec processing software.[43] Relative abundances of the charge states were used to calculate a weighted average charge. All experiments were conducted on the Thermo Q Exactive UHMR (ultra-high mass range) instrument. Mass resolution was set to either 6250 or 12500 for all experiments shown here. Instrument tuning conditions used to promote desolvation of ions were maintained at identical levels for each protein complex to provide an accurate comparison of charge reduction that are solely dependent on solution conditions. Spray voltage was also tuned to achieve highest signal except in the experiments where spray voltage was used as the variable in the experiment. Spray voltage is defined as the absolute voltage measured on the emitter referenced to ground. Heated capillary temperatures were maintained at 200 °C.

Triplicate collisional-cross section (CCS) measurements for CRP were made using mixed buffer solutions with varying ratios of AmAc and TEAA; 200 mM AmAc or 160 mM AmAc with 0, 5, 10, or 15 mM TEAA. The emitter potentials were tuned to get optimal signal and then biased by ~+200 V and ~+400 V relative to initial voltage to explore the CSD sampled at higher emitter voltages. Ion mobility experiments were conducted using the Fourier transform periodic-focusing ion-mobility drift tub (FT-PF-IM-DT) UHMR Orbitrap instrument. All experiments were performed using helium collision gas at 1.725 torr, at 23.7 °C. A more detailed description of the fundamental theory and workings of the instrument has been described thoroughly in previous papers.[44–47]

Results

To explore the effects of charge reduction on protein complexes, various mixtures of TEAA and AmAc were screened against 3 protein complexes (CRP, PK, and GDH). The observations from this study led to the conclusion that as the concentration of TEAA was increased, the Z_{avg} of the observed charge state distribution was lowered. This trend reached asymptotal behavior beginning at 20 mM TEAA. Figure 1A summarizes the average charge state of 3 protein complexes (CRP, PK, and GDH) in response to different concentrations of TEAA.

Emitter voltages can vary based on various solution factors and can be used to control the ionization efficiency. For certain buffer conditions, increased nESI emitter voltage caused

a shift to a lower charge state for proteins in mixed buffer conditions. The mass spectra clearly show a large change in charge state distribution (CSD) in response to an increase in the emitter potential of about +400 V from the initial nESI potential (see Figure S1 in Supporting Information). Figure 1A reveals two different trends for the Z_{avg} for each protein complex studied: 1) an increase in emitter potential lowers the Z_{avg} of the ions for a given set of buffer conditions; 2) as TEAA concentration is increased the emitter potential needed to lower the Z_{avg} of the ions decreases. The plots in Figures 1B and 1C show both trends; Figure 1B shows the observed change in relative abundance for the low and high CSDs as a function of emitter voltage while **1C** shows the change in CSD as a function of TEAA concentration. The AmAc concentration was maintained at 160 mM regardless of the TEAA concentration. This was intended to keep a fixed concentration of AmAc in the solution even though that as the concentration of TEAA was varied the ionic strength of the solution would be altered as well. The concentration of AmAc did not have a significant effect in subsequent trials (data not shown) and reaffirmed the observation that TEAA concentration was responsible for charge reduction.

The mass spectra of CRP, PK, and GDH in 10 mM TEAA and 160 mM AmAc (Figure 2) show bimodal CSDs; these bimodal distributions are due to the presence of two different ion populations and suggest that there are two ionization mechanisms operating to generate each ion population. The higher Z_{avg} distribution is similar to that seen when sprayed from an AmAc solution whereas the lower Z_{avg} distribution is similar to results seen in a mixed buffer solution containing higher concentrations of TEAA (*e.g.*, > 20 mM TEA, see Figure 1 and Figure S2). This bimodal CSD behavior dissipates at higher concentrations of TEAA in the solution and at higher nESI emitter potentials. The distributions are sensitive to emitter potentials and can be shifted reversibly to higher or lower charge states by changing the bias placed on the nESI emitter (Figure S3). At 20 mM TEAA, the ion populations of these protein complexes are nearly entirely charge-reduced. This observation implies that a critical concentration of TEAA in the droplet is necessary to effectively charge reduce the ions, and that there exists a small concentration window to observe the shift in Z_{avg} from non-charge-reduced to charge-reduced distributions. The emitter potential effects suggest that higher spray voltages increase the partitioning of surface-active charge carries between the bulk and the surface of the nanodroplet. This would explain why lower Z_{avg} are observed at higher emitter potentials without increasing the bulk concentration of charge reducing reagents in the solution.

Trialkylamines and diaminoalkanes were added to AmAc solutions to explore the effect of surface activity on the efficacy of charge reduction. The final concentrations for these solutions consisted of 40 mM of selected amine and 160 mM of ammonium acetate. Figure 3A contains the high *m/z* range of mass spectra obtained using solution with and without added charge reducing buffers. TMA, TEAA, and TPA show increased ability to reduce the Z_{avg} for both GDH and CRP concomitantly with the increasing lengths of the alkane chains. Similar data (Figure 3B) were obtained using 1,7-DAH solution, which is even more effective for lowering the Z_{avg} of the CRP ions than the 1,6-DAH and 1,5-DAP solutions. Increasing the length of the alkane chains increases the hydrophobicity and in turn the surface activity of these charge carriers thus decreasing the favorability of being solvated in

the “bulk” solution of the droplet. This is also demonstrated when comparing the exhibited charge reduction of the alkyl diammonium series and the trialkylammonium series for CRP. The trialkylammonium ions are more effective at reducing the Z_{avg} of CRP because they are more hydrophobic than the alklyl diammonium ions. The emission of these molecules from the droplet is responsible for the lower Z_{avg} of the resulting macromolecular ions exhibited in Figure 3.

Discussion

Surface-activity is a term used here to describe how likely hydrophobic charge carriers, *e.g.*, alkylamines, are to be partitioned to the surface of the nanodroplet. The initial understanding of how charge is distributed in charged nanodroplets is attributed to Gauss’ law which predicts that charges are located at the surface of the droplet due to coulombic repulsion. Simulations conducted by Konermann *et al.* demonstrated that small charge carriers (Na^+, K^+, NH_4^+) are preferentially solvated and that their existence at the surface of the droplet would bear an enthalpic penalty.[27, 48, 49] On the other hand, larger hydrophobic charge carriers that are less preferentially solvated would be partitioned to the surface of the droplet more than smaller ions. Hogan *et al.* describe a process by which surface active ions are ejected from the droplet before CRM formation of the macromolecular ion.[36] These surface active ions are preferentially ejected from the droplet leading to lower charge states for the respective macromolecules. With more surface-active charge carriers being emitted from the droplet, fewer charges are then available to reside on the macromolecule. The CC-FEM, in essence, is the mechanism underlying the charge reduction of protein ions generated from nESI. Figure 4 presents the CC-FEM mechanism (**A**) along with the CRM (**B**) for comparison. Bush *et al.* concluded that a CC-FEM model is also applicable to negative mode electrosprays inclusively.[50] They showed that negative charge carriers can more easily be emitted from the droplet than positive charge carriers, resulting in lower overall charge for negative ions. A possible aside to the CC-FEM is the effect that droplet surface tension may have on the final charge state of gas-phase ions. Donald *et al.* observed trends in supercharging effects on proteins (i.e., increased Z_{avg}) while using cyclic alkyl carbonates and cyclic alkyl sulphites, with various alkyl chain lengths, as supercharging reagents.[51]

The data presented in Figure 3 demonstrate the surface activity effect described by the CC-FEM. Protein ions generated from these mixed buffer conditions are more charge-reduced in the presence of buffer components that are more surface active. As an example, TMA is much more easily solvated than TPA; thus, TPA is more surface active and much easier to eject from the nanodroplet. Therefore, the Z_{avg} for proteins in TPA solutions is much lower than that for TMA. This same effect applies to the alkyl diammonium series. The increased length of the alkyl chain increases the surface activity of the molecule and is responsible for the observed charge reduction effects. It is interesting to note the slight differences in the charge reduction effects between the classes of diammonium alkanes. The CSD for CRP in a 40 mM TPA, 160 mM AmAc solution is centered around the 16^+ and 17^+ charge states, whereas the CSD for CRP in a 40 mM 1,7-DAH, 160 mM AmAc solution produces a CSD centered around the 18^+ charge state. 1,7-DAH ions are less surface active than the TPA ions and therefore are not as effective at charge reducing ions. The addition of these amino-containing compounds to the solution did not produce observable signs of protein

instability (*i.e.*, dissociation of protein complexes) for the specific conditions used in these experiments (Figure S4).

Gas-phase basicities of amines are well studied and characterized,[52] and it has been proposed that gas-phase basicities are determinants of protein charge reduction in ESI.[18, 19, 52–54] While gas-phase basicity may play a role in the mechanism of charge reduction, the observations pertaining to the bimodality of protein ion CSDs do not support this argument.[36] Gas-phase proton transfer reactions from the protein to an amine would be expected to yield a uniform distribution of charge states that would decrease as the concentration of the gas-phase base increased. While gas-phase proton transfers have been demonstrated to charge reduce ions,[55, 56] it is unlikely that gas-phase proton transfers are responsible for charge reduction via a single ESI emitter owing to the short time scales available in transit to the mass spectrometer and the low densities of ions with which these transfers would be required to occur. Hogan et al. predicted and observed that a bimodal distribution of protein charge state distributions would occur in a mixed buffer environment if charge emission from the droplet was responsible for the observed charge reduction.[36] The initial progeny droplets produced from the mother droplet would be enriched in surface active charge carriers. However, if the overall concentration of charge reduction reagents becomes diminished due to repeated fissioning of the droplet, later progeny droplets produced from that same mother droplet would receive fewer surface-active ions to remove charges from the nanodroplet. This, in turn, would give rise to protein ion populations with bimodal charge state distributions, charge reduced populations from earlier fission events and non-charge reduced populations from late fission events.

Bimodal charge state distributions were also observed for GDH, CRP, and PK in multiple concentrations of TEAA-containing buffers in Figure 2. The formation of nonspecific dimers for these protein complexes was observed and was initially considered to be the source of these charge reduced ions. However, the breakup of dimer ions does not account for the solution- and voltage-dependance that are observed is these experiments. The conditions needed to bring about the charge reduction were controlled by varying the nESI emitter potential and the TEAA concentration present in the buffer. As seen in Figure 1, the Z_{avg} of the protein complexes was sensitive to the concentration of TEAA present in the solution. The emitter potential was also used to increase the relative concentration of TEAA in the droplet. Support for this may be drawn from the observation that higher emitter potentials are linked to larger initial droplet sizes.[57] This may provide increased enrichment of surface active charge carriers in progeny droplets.[10, 58] The need to increase the emitter voltage to effectively lower the charge state distributions of the ions demonstrates that a critical concentration of TEAA is necessary in the droplet to bring about charge reduction of the protein ions.

It is clear from Figure 2 that these conditions show the transitory steps from a non-charge-reduced ion population to a charge-reduced population. These data also exhibit the predicted effects outlined by a field emission mechanism as being responsible for charge reduction rather than it being entirely dependent on gas-phase basicity. Lastly, as the TEAA concentration was increased beyond the limit necessary to begin generating charge-reduced

macromolecular ions, the field emission mechanism takes over as the concentration of surface-active ions is sufficient to remove excess charges from the subsequent nanodroplets.

Figure 5 shows the change in CCS across the different sets of solution conditions and emitter potentials for each charge state measured. Two observations were made: 1) when compared among conditions for the same charge state, the CCS does not change significantly; 2) the emitter potential, while decreasing the charge state, did not decrease the CCS when compared to other conditions for that charge state. This would indicate that the observed charge reduction is not a consequence of conformational change induced by the charge reduction reagents.

Charge states of proteins and protein complexes in nMS are closely linked to the solvent-accessible surface area (SASA) of the proteins.[59, 60] It is often appropriate to correlate the charge state of the protein to the conformational state of the protein, i.e., whether the protein has adopted a more native-like or more extended/unfolded state; higher charge states of proteins are indicative of more extended structures.[24] The question arises, are charge reduction reagents reducing charge states of proteins by altering conformation(s) or are they only perturbing the ESI process? Ion mobility measurements would be able to offer insight into this question. The CCS values shown in Figure 5 clearly show that TEAA concentration does not promote statistically significant changes in CCS for the protein CRP (CCS values and IMS conditions can be found in Table S1). Even higher emitter voltages, while decreasing the average charge state, do not reduce the CCS when compared to other solution conditions for the same charge state. The lower charge states have lower CCS, which would be explained by a reduction in the coulombic repulsion in the ion. These results support the idea that TEAA reduces average charge states via an ESI mechanism without influencing the conformational preference of the protein ions.

Conclusion

The results presented here provide additional experimental evidence for the dual ionization model, CC-FEM, for formation of protein complex ions via nESI. This model provides a rationalization for the observed phenomena of charge state reduction in mixed buffer solutions, *viz.* surface activity of the charge-carrying molecules in the nanodroplet definitively predicts the efficacy of the molecule to induce charge reduction of macromolecular ions. Higher emitter potentials are responsible for producing lower charge states of proteins by increasing the partition of surface-active ions in the nanodroplet, forcing surface active ions to the droplet surface. Bimodal charge state distributions for proteins indicate that charge emission of surface-active ions, rather than a gas-phase proton transfer, is responsible for charge reduction. The observed effects of solution composition and ESI conditions apply also to monomeric proteins. We chose to focus this study on protein complexes due to higher innate charge which illustrates the effect of charge reduction more distinctly.

Protein charge states in native MS are linked to the SASA of the protein. Lower protein charge states favor more native-like conformations in the gas phase due to a reduction in coulombic repulsion.[22–24] It is important to understand how the components in the

solution interact with the protein to provide a more accurate framework in which to interpret experimental observations. In these studies, the diaminoalkane molecules were observed to increase the width of the charge state distribution for CRP, which is a potential indicator of conformational drift; however, the CCS for CRP suggest otherwise. These questions illustrate the needs for additional studies on these processes, specifically surface-induced dissociation (SID).[61, 62] Here we do not address potential effects of co-solutes that may also alter the charge states of protein complexes, specifically osmolytes and chaperones. As noted previously for TMAO,[19] these co-solutes are more likely to induce significant compositional and conformational changes. Studies addressing these issues are currently underway.

Supplementary Material

Refer to Web version on PubMed Central for supplementary material.

Acknowledgment

Funding for this work was provided by the National Institutes of Health grants P41GM128577 (DHR), R01GM138863 (DHR, AL), and R44GM133239 (DHR, AL).

References

1. Yamashita M; Fenn JB, Electrospray Ion-Source - Another Variation on the Free-Jet Theme. J Phys Chem-Us 1984, 88 (20), 4451–4459.
2. Yamashita M; Fenn JB, Negative-Ion Production with the Electrospray Ion-Source. J Phys Chem-Us 1984, 88 (20), 4671–4675.
3. Whitehouse CM; Dreyer RN; Yamashita M; Fenn JB, Electrospray interface for liquid chromatographs and mass spectrometers. Anal Chem 1985, 57 (3), 675–9. [PubMed: 2581476]
4. Fenn JB; Mann M; Meng CK; Wong SF; Whitehouse CM, Electrospray Ionization-Principles and Practice. Mass Spectrometry Reviews 1990, 9 (1), 37–70.
5. Iavarone AT; Williams ER, Supercharging in electrospray ionization: effects on signal and charge. International Journal of Mass Spectrometry 2002, 219 (1), 63–72.
6. Yin S; Loo JA, Top-Down Mass Spectrometry of Supercharged Native Protein-Ligand Complexes. Int J Mass Spectrom 2011, 300 (2–3), 118–122. [PubMed: 21499519]
7. Nshanian M; Lakshmanan R; Chen H; Ogorzalek Loo RR; Loo JA, Enhancing Sensitivity of Liquid Chromatography-Mass Spectrometry of Peptides and Proteins Using Supercharging Agents. Int J Mass Spectrom 2018, 427, 157–164. [PubMed: 29750076]
8. Konermann L, Addressing a Common Misconception: Ammonium Acetate as Neutral pH “Buffer” for Native Electrospray Mass Spectrometry. J Am Soc Mass Spectrom 2017, 28 (9), 1827–1835. [PubMed: 28710594]
9. Limbach PA; Crain PF; McCloskey JA, Molecular mass measurement of intact ribonucleic acids via electrospray ionization quadrupole mass spectrometry. J Am Soc Mass Spectrom 1995, 6 (1), 27–39. [PubMed: 24222058]
10. Xia Z; DeGrandchamp JB; Williams ER, Native mass spectrometry beyond ammonium acetate: effects of nonvolatile salts on protein stability and structure. Analyst 2019, 144 (8), 2565–2573. [PubMed: 30882808]
11. Susa AC; Xia Z; Williams ER, Native Mass Spectrometry from Common Buffers with Salts That Mimic the Extracellular Environment. Angew Chem Int Ed Engl 2017, 56 (27), 7912–7915. [PubMed: 28510995]
12. Susa AC; Xia Z; Tang HYH; Tainer JA; Williams ER, Charging of Proteins in Native Mass Spectrometry. J Am Soc Mass Spectrom 2017, 28 (2), 332–340. [PubMed: 27734326]

13. Pacholarz KJ; Garlish RA; Taylor RJ; Barran PE, Mass spectrometry based tools to investigate protein-ligand interactions for drug discovery. Chem Soc Rev 2012, 41 (11), 4335–55. [PubMed: 22532017]
14. Ruotolo BT; Benesch JL; Sandercock AM; Hyung SJ; Robinson CV, Ion mobility-mass spectrometry analysis of large protein complexes. Nat Protoc 2008, 3 (7), 1139–52. [PubMed: 18600219]
15. Hernandez H; Robinson CV, Determining the stoichiometry and interactions of macromolecular assemblies from mass spectrometry. Nat Protoc 2007, 2 (3), 715–26. [PubMed: 17406634]
16. Heck AJ; Van Den Heuvel RH, Investigation of intact protein complexes by mass spectrometry. Mass Spectrom Rev 2004, 23 (5), 368–89. [PubMed: 15264235]
17. Kebarle P; Verkerk UH, Electrospray: from ions in solution to ions in the gas phase, what we know now. Mass Spectrom Rev 2009, 28 (6), 898–917. [PubMed: 19551695]
18. Stiving AQ; Jones BJ; Ujma J; Giles K; Wysocki VH, Collision Cross Sections of Charge-Reduced Proteins and Protein Complexes: A Database for Collision Cross Section Calibration. Anal Chem 2020, 92 (6), 4475–4483. [PubMed: 32048834]
19. Lyu J; Liu Y; McCabe JW; Schrecke S; Fang L; Russell DH; Laganowsky A, Discovery of Potent Charge-Reducing Molecules for Native Ion Mobility Mass Spectrometry Studies. Anal Chem 2020, 92 (16), 11242–11249. [PubMed: 32672445]
20. Zhou M; Dagan S; Wysocki VH, Impact of charge state on gas-phase behaviors of noncovalent protein complexes in collision induced dissociation and surface induced dissociation. Analyst 2013, 138 (5), 1353–62. [PubMed: 23324896]
21. Pacholarz KJ; Barran PE, Use of a charge reducing agent to enable intact mass analysis of cysteine-linked antibody-drug-conjugates by native mass spectrometry. EuPA Open Proteom 2016, 11, 23–27. [PubMed: 29900109]
22. Pagel K; Hyung SJ; Ruotolo BT; Robinson CV, Alternate dissociation pathways identified in charge-reduced protein complex ions. Anal Chem 2010, 82 (12), 5363–72. [PubMed: 20481443]
23. Mehmood S; Marcoux J; Hopper JT; Allison TM; Liko I; Borysik AJ; Robinson CV, Charge reduction stabilizes intact membrane protein complexes for mass spectrometry. J Am Chem Soc 2014, 136 (49), 17010–2. [PubMed: 25402655]
24. Hall Z; Politis A; Bush MF; Smith LJ; Robinson CV, Charge-state dependent compaction and dissociation of protein complexes: insights from ion mobility and molecular dynamics. J Am Chem Soc 2012, 134 (7), 3429–38. [PubMed: 22280183]
25. Dyachenko A; Gruber R; Shimon L; Horovitz A; Sharon M, Allosteric mechanisms can be distinguished using structural mass spectrometry. Proc Natl Acad Sci U S A 2013, 110 (18), 7235–9. [PubMed: 23589876]
26. Ahadi E; Konermann L, Ejection of solvated ions from electrosprayed methanol/water nanodroplets studied by molecular dynamics simulations. J Am Chem Soc 2011, 133 (24), 9354–63. [PubMed: 21591733]
27. Konermann L; Ahadi E; Rodriguez AD; Vahidi S, Unraveling the mechanism of electrospray ionization. Anal Chem 2013, 85 (1), 2–9. [PubMed: 23134552]
28. Aliyari E; Konermann L, Formation of Gaseous Proteins via the Ion Evaporation Model (IEM) in Electrospray Mass Spectrometry. Anal Chem 2020, 92 (15), 10807–10814. [PubMed: 32610010]
29. Iribarne JV, On the evaporation of small ions from charged droplets. The Journal of Chemical Physics 1976, 64 (6).
30. Loscertales IG; Fernández de la Mora J, Experiments on the kinetics of field evaporation of small ions from droplets. The Journal of Chemical Physics 1995, 103 (12), 5041–5060.
31. delaMora JF, On the outcome of the coulombic fission of a charged isolated drop. J Colloid Interf Sci 1996, 178 (1), 209–218.
32. Martin LM; Konermann L, Enhancing Protein Electrospray Charge States by Multivalent Metal Ions: Mechanistic Insights from MD Simulations and Mass Spectrometry Experiments. J Am Soc Mass Spectrom 2020, 31 (1), 25–33. [PubMed: 32881517]
33. Metwally H; Duez Q; Konermann L, Chain Ejection Model for Electrospray Ionization of Unfolded Proteins: Evidence from Atomistic Simulations and Ion Mobility Spectrometry. Anal Chem 2018, 90 (16), 10069–10077. [PubMed: 30040388]

34. Consta S, Fragmentation reactions of charged aqueous clusters. J Mol Struc-Theochem 2002, 591, 131–140.
35. Harper CC; Brauer DD; Francis MB; Williams ER, Direct observation of ion emission from charged aqueous nanodrops: effects on gaseous macromolecular charging. Chem Sci 2021, 12 (14), 5185–5195. [PubMed: 34168773]
36. Hogan CJ Jr.; Carroll JA; Rohrs HW; Biswas P; Gross ML, Combined charged residue-field emission model of macromolecular electrospray ionization. Anal Chem 2009, 81 (1), 369–77. [PubMed: 19117463]
37. Davidovic M; Mattea C; Qvist J; Halle B, Protein Cold Denaturation as Seen From the Solvent. Journal of the American Chemical Society 2009, 131 (3), 1025–1036. [PubMed: 19115852]
38. Gamero-Castano M; de la Mora JF, Mechanisms of electrospray ionization of singly and multiply charged salt clusters. Anal Chim Acta 2000, 406 (1), 67–91.
39. Gamero-Castano M; Mora JF, Kinetics of small ion evaporation from the charge and mass distribution of multiply charged clusters in electrosprays. J Mass Spectrom 2000, 35 (7), 790–803. [PubMed: 10934433]
40. Hogan CJ Jr.; de la Mora JF, Ion mobility measurements of nondenatured 12–150 kDa proteins and protein multimers by tandem differential mobility analysis-mass spectrometry (DMA-MS). J Am Soc Mass Spectrom 2011, 22 (1), 158–72. [PubMed: 21472554]
41. Hogan CJ Jr.; Carroll JA; Rohrs HW; Biswas P; Gross ML, Charge carrier field emission determines the number of charges on native state proteins in electrospray ionization. J Am Chem Soc 2008, 130 (22), 6926–7. [PubMed: 18461930]
42. Walker TE; Shirzadeh M; Sun HM; McCabe JW; Roth A; Moghadamchargari Z; Clemmer DE; Laganowsky A; Rye H; Russell DH, Temperature Regulates Stability, Ligand Binding (Mg(2+) and ATP), and Stoichiometry of GroEL-GroES Complexes. J Am Chem Soc 2022, 144 (6), 2667–2678. [PubMed: 35107280]
43. Marty MT; Baldwin AJ; Marklund EG; Hochberg GK; Benesch JL; Robinson CV, Bayesian deconvolution of mass and ion mobility spectra: from binary interactions to polydisperse ensembles. Anal Chem 2015, 87 (8), 4370–6. [PubMed: 25799115]
44. Silveira JA; Jeon J; Gamage CM; Pai PJ; Fort KL; Russell DH, Damping factor links periodic focusing and uniform field ion mobility for accurate determination of collision cross sections. Anal Chem 2012, 84 (6), 2818–24. [PubMed: 22404635]
45. Poltash ML; McCabe JW; Patrick JW; Laganowsky A; Russell DH, Development and Evaluation of a Reverse-Entry Ion Source Orbitrap Mass Spectrometer. J Am Soc Mass Spectrom 2019, 30 (1), 192–198. [PubMed: 29796735]
46. Poltash ML; McCabe JW; Shirzadeh M; Laganowsky A; Clowers BH; Russell DH, Fourier Transform-Ion Mobility-Orbitrap Mass Spectrometer: A Next-Generation Instrument for Native Mass Spectrometry. Anal Chem 2018, 90 (17), 10472–10478. [PubMed: 30091588]
47. McCabe JW; Mallis CS; Kocurek KI; Poltash ML; Shirzadeh M; Hebert MJ; Fan L; Walker TE; Zheng X; Jiang T; Dong S; Lin CW; Laganowsky A; Russell DH, First-Principles Collision Cross Section Measurements of Large Proteins and Protein Complexes. Anal Chem 2020, 92 (16), 11155–11163. [PubMed: 32662991]
48. Metwally H; McAllister RG; Popa V; Konermann L, Mechanism of Protein Supercharging by Sulfolane and m-Nitrobenzyl Alcohol: Molecular Dynamics Simulations of the Electrospray Process. Anal Chem 2016, 88 (10), 5345–54. [PubMed: 27093467]
49. Ahadi E; Konermann L, Surface charge of electrosprayed water nanodroplets: a molecular dynamics study. J Am Chem Soc 2010, 132 (32), 11270–7. [PubMed: 20698694]
50. Allen SJ; Schwartz AM; Bush MF, Effects of polarity on the structures and charge states of native-like proteins and protein complexes in the gas phase. Anal Chem 2013, 85 (24), 12055–61. [PubMed: 24224685]
51. Foley EDB; Zenaidee MA; Tabor RF; Ho J; Beves JE; Donald WA, On the mechanism of protein supercharging in electrospray ionisation mass spectrometry: Effects on charging of additives with short- and long-chain alkyl constituents with carbonate and sulphite terminal groups. Anal Chim Acta X 2019, 1, 100004. [PubMed: 33186415]

52. Tang M; Isbell J; Hedges B; Brodbelt J, Comparison of Gas-Phase Basicities and Ion-Molecule Reactions of Aminobenzoic Acids. Journal of Mass Spectrometry 1995, 30 (7), 977–984.

53. Catalina MI; van den Heuvel RH; van Duijn E; Heck AJ, Decharging of globular proteins and protein complexes in electrospray. Chemistry 2005, 11 (3), 960–8. [PubMed: 15593239]

54. Iavarone AT; Jurchen JC; Williams ER, Effects of solvent on the maximum charge state and charge state distribution of protein ions produced by electrospray ionization. J Am Soc Mass Spectrom 2000, 11 (11), 976–85. [PubMed: 11073261]

55. Foreman DJ; McLuckey SA, Recent Developments in Gas-Phase Ion/Ion Reactions for Analytical Mass Spectrometry. Anal Chem 2020, 92 (1), 252–266. [PubMed: 31693342]

56. Stutzman JR; Bain RM; Hagenhoff S; Woodward WH; O'Brien JP; Lesniak M, Microdroplet Fusion Chemistry for Charge State Reduction of Synthetic Polymers via Bipolar Dual Spray with Anionic Reagents. J Am Soc Mass Spectrom 2019, 30 (9), 1742–1749. [PubMed: 31140078]

57. Davidson KL; Oberreit DR; Hogan CJ; Bush MF, Nonspecific aggregation in native electrokinetic nanoelectrospray ionization. International Journal of Mass Spectrometry 2017, 420, 35–42.

58. Xia Z; Williams ER, Effect of droplet lifetime on where ions are formed in electrospray ionization. Analyst 2018, 144 (1), 237–248. [PubMed: 30488074]

59. Konermann L; Silva EA; Sogbein OF, Electrochemically induced pH changes resulting in protein unfolding in the ion source of an electrospray mass spectrometer. Anal Chem 2001, 73 (20), 4836–44. [PubMed: 11681459]

60. Benesch JLP; Sobott F; Robinson CV, Thermal dissociation of multimeric protein complexes by using nanoelectrospray mass spectrometry. Analytical Chemistry 2003, 75 (10), 2208–2214. [PubMed: 12918957]

61. Snyder DT; Harvey SR; Wysocki VH, Surface-induced Dissociation Mass Spectrometry as a Structural Biology Tool. Chem Rev 2022, 122 (8), 7442–7487. [PubMed: 34726898]

62. Stiving AQ; VanAernum ZL; Busch F; Harvey SR; Sarni SH; Wysocki VH, Surface-Induced Dissociation: An Effective Method for Characterization of Protein Quaternary Structure. Anal Chem 2019, 91 (1), 190–209. [PubMed: 30412666]

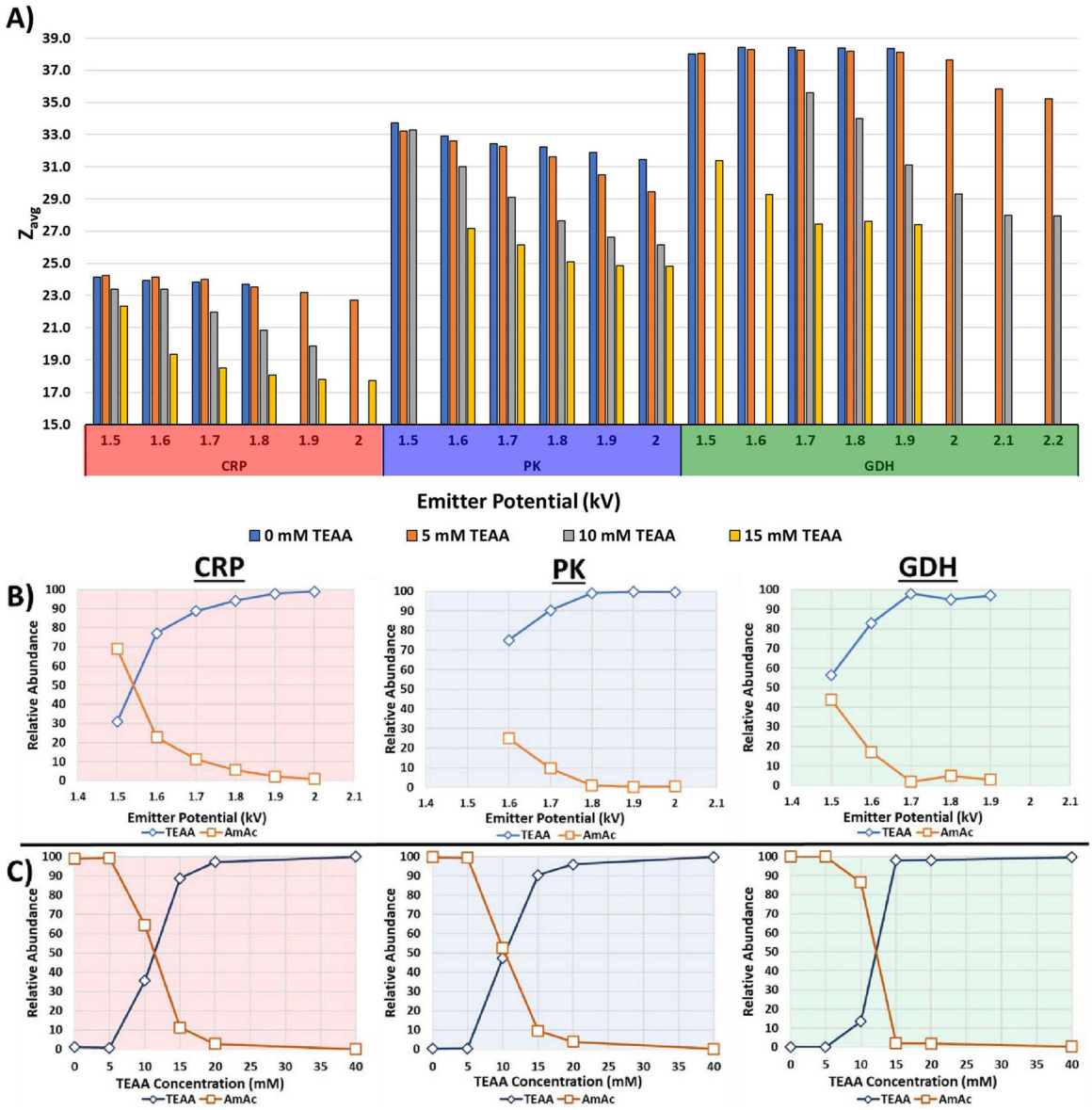

Figure 1.

A) Bar charts displaying the average charge state of CRP, PK, and GDH protein complexes as a function of TEAA concentration and emitter voltage. The Z_{avg} shifts by up as much as 25% simply by increasing spray voltage. AmAc concentrations are held constant at 160 mM for all data in this figure. **B)** Plots showing the relative abundances of the low (TEAA-like) and high (AmAc-like) CSDs for 15 mM TEAA and 160 mM AmAc buffer conditions as a function of emitter potential. **C)** These plots show the same information as **(B)** but as a function of TEAA concentration at 1.7 kV emitter potential.

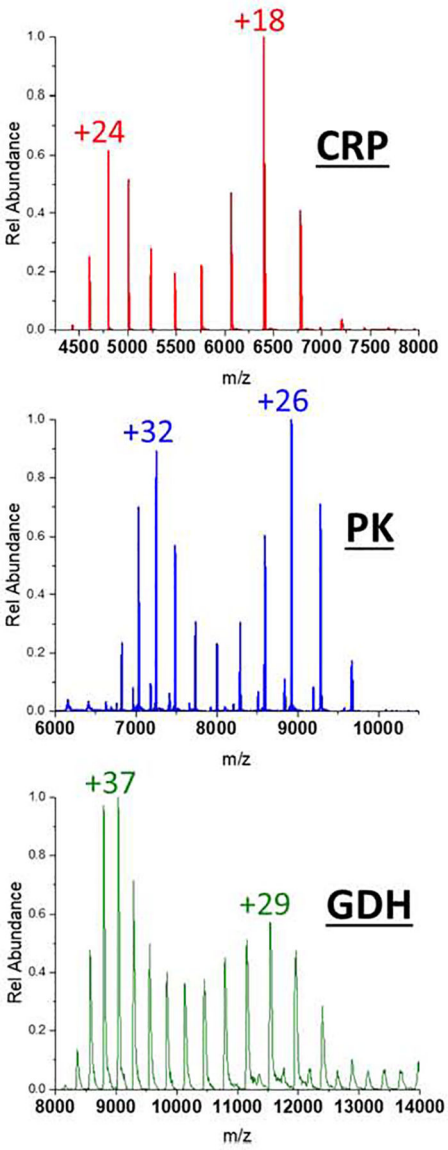

Figure 2.

Mass spectra of CRP, PK, and GDH demonstrating the bimodal charge state distribution that accompanies a combined ionization model. The higher charge state distributions are typical for AmAc buffers, whereas the lower charge state distributions are typical for TEAA charge reduction. The buffer concentrations are 10 mM TEAA and 160 mM AmAc.

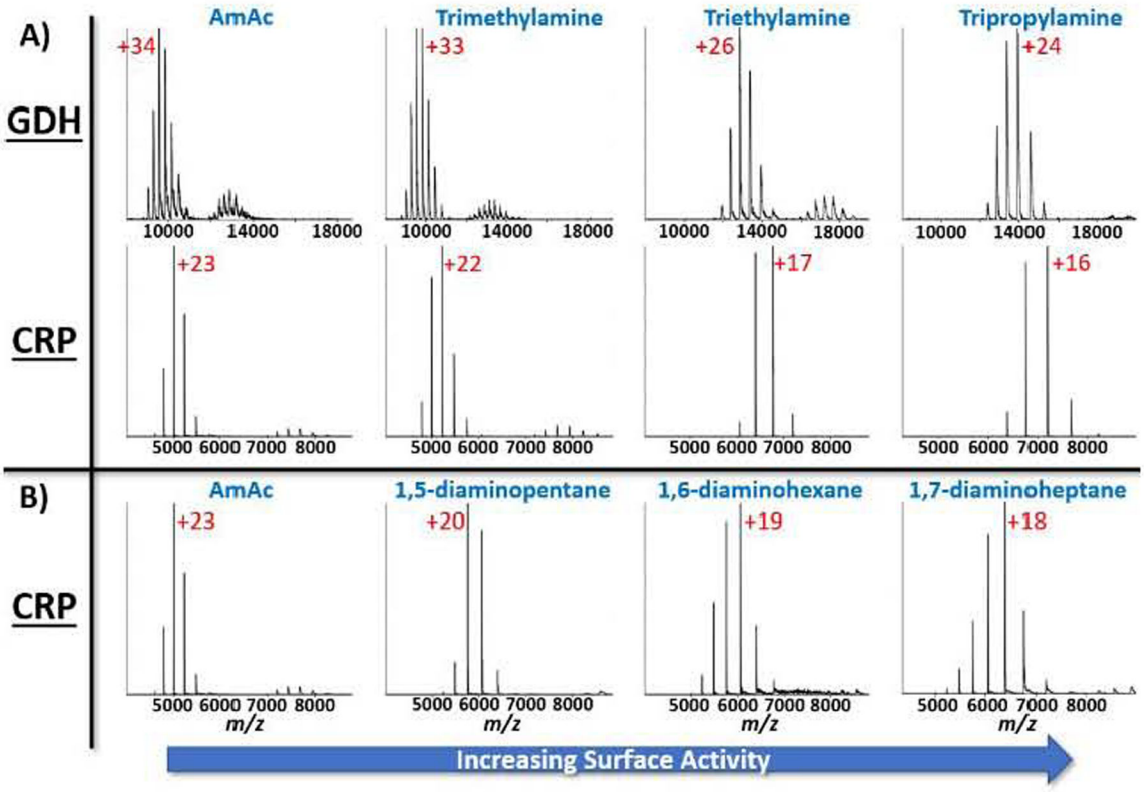

Figure 3.

Mass spectra demonstrating the efficacy of amines and dialkylamines to reduce the Z_{avg} of given proteins. **A)** GDH and CRP protein solutions had 40 mM of a given amine added to the solution. For both protein complexes a trend of lower Z_{avg} exists as the surface activity of the amine increases. **B)** CRP mass spectra in a similar experiment using dialkylamines to show a trend of increasing charge reduction as the surface activity of the dialkylamine increases. Once again, the most surface-active charge carrier is the most effective charge reduction agent. Labeled charge state are the charge state of the peak with the highest relative abundance.

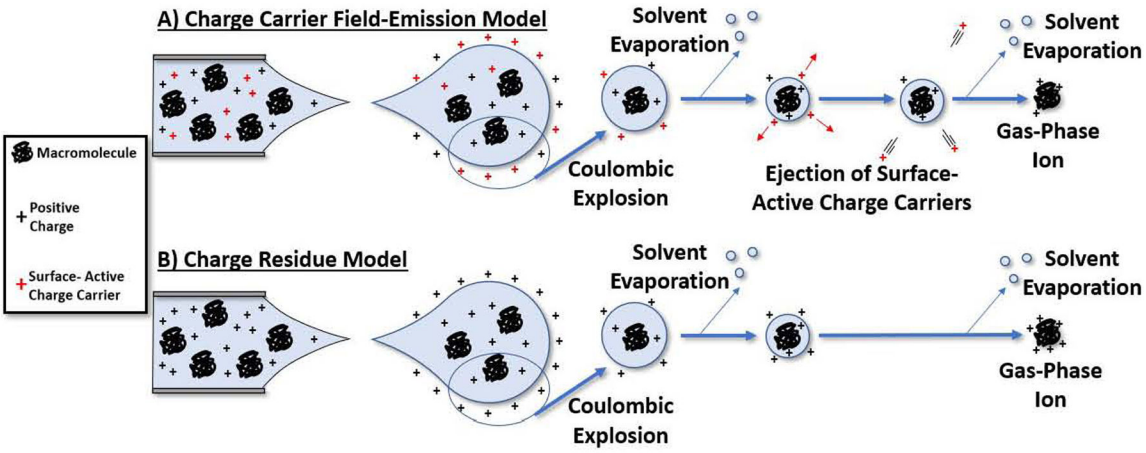

Figure 4.

A) A representative sketch of the basic mechanism for combined CRM and IEM. Surface active charge carriers disproportionally populate the surface of the parent droplet. Progeny droplets then are given large relative concentrations of surface-active charge carriers. These charge carriers leave the droplet and syphon excess charges from the droplet. The proteins left in the nanodroplet are then ionized via a CRM pathway. **B)** The CRM is generally accepted as the mechanism for the formation of macromolecular ions from ESI droplets. The charge carriers in this model are more likely to stay solvated in solution and thus their charge will become deposited upon loss of the solvent.

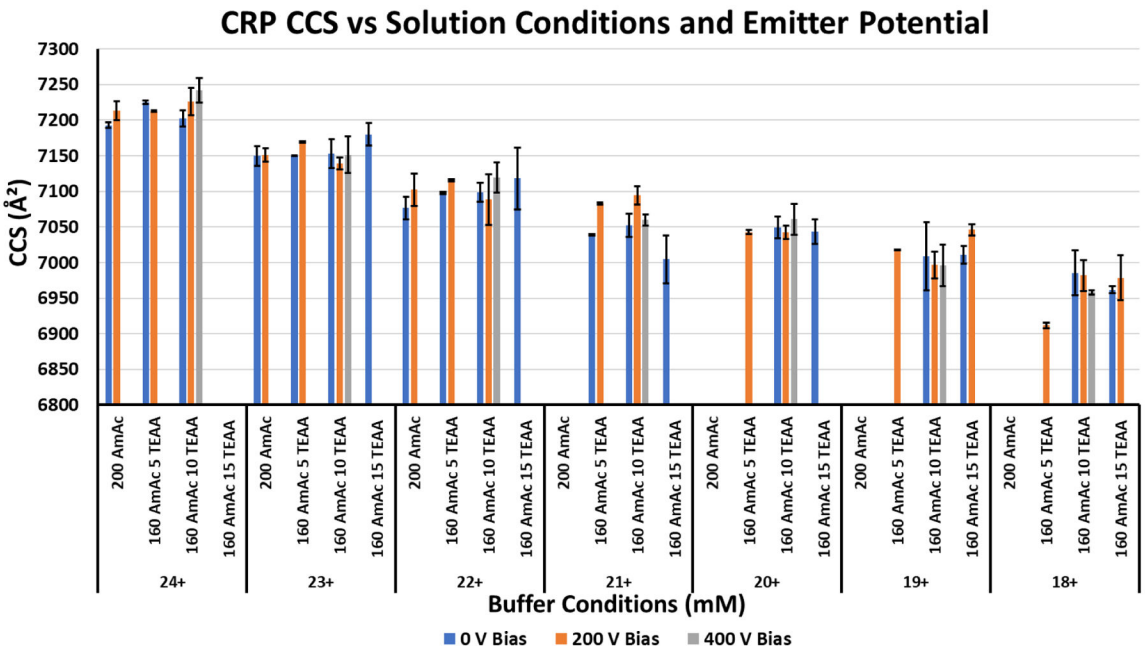

Figure 5.

Bar chart for the measured CCS of CRP from different charge reducing solutions and nESI emitter potentials. Black error bars delineate the standard deviation of triplicate measurements. Variations in the buffer do not change the CCS significantly when compared among other conditions for the same charge state. Despite lowering the average charge state, higher emitter voltages did not change the CCS values significantly when compared to other values for the same charge state. These results are evidence that the TEAA concentration is not influencing the conformational preference of the protein complex when compared to the same charge state under other buffer conditions.